TRANSONIC FLUTTER ANALYSIS OF AN AIRFOIL WITH APPROXIMATE BOUNDARY METHOD

Zhu Biao, Qiao Zhide, Gao Chao
The Center for Aerodynamic Design and Research, Northwestern Polytechnical University, Xi'an, China, 710072

Keywords: *approximate boundary conditions, Cartesian grids, flutter, Euler equations*

Abstract

Numerical simulation of aircraft's flutter is rather expensive and time-consuming. In order to save expense and calculating time, we apply first-order approximate conditions to solve the unsteady transonic Euler equations coupled with aeroelastic equations. Assuming that the airfoil is thin and undergoes small deformation, we implement wall boundary conditions on non-moving mean wall positions. Then the first-order approximate equation of momentum is obtained by using Taylor expansion. Unsteady transonic Euler equations are solved on stationary Cartesian grids.

Calculation of the aerodynamic behavior is performed for NACA 64A010 airfoil in transonic flow, while the flutter boundaries of AGARD wing model and NACA 0012 benchmark model are calculated for aeroelastic simulation. The results are in good agreement with other numerical and experimental results, preliminarily indicating that the first-order approximate conditions are effective for aeroelastic simulation.

1 Introduction

Aeroelastic simulation, such as flutter prediction, is an important issue for modern aircraft design. If flutter occurs during flight, it will be lead to disastrous structural failure. So flutter is a catastrophic aeroelastic phenomenon that all flight vehicles must be clear of in their flight envelope.

Over the last decade, significant progress has been made on developing numerical methods for the solution of Euler and N-S equations. Bendiksen and Kousen[1,2] used an explicit time accurate two-dimensional Euler code to study the nonlinear effects in transonic flutter. With their model, they demonstrated the possibility of LCO in a transonic flow. Lee-Rausch and Batina[3,4] developed three-dimensional methods for the Euler and Navier-Stokes equations, respectively, for predicting the flutter boundaries of wings. Alonso and Jameson[5] developed a model which is close to the fully coupled method by solving unsteady Euler equations coupled structural equations. Liu[6] developed a fully coupled method using Jameson's explicit scheme with multigrid method and a finite element structural model. The grids for CFD solver have to be regenerated in total computational field at every real time step, however the grid generating is a time consuming work. So we have to use some new numerical method for aeroelastic simulation to decreasing the calculating time and increasing the calculating efficiency, meanwhile keeping the required precision.

In this paper, we solve the unsteady Euler equations coupled with structural equations by using the first-order approximate boundary conditions[7,8,9] to simulate the airfoil's aeroelasticity. Cell-center finite volume method spatial derivatives, implicit dual-time temporal derivatives and 5-step Runge-Kutta scheme are adopted in the solution of unsteady flow. The techniques of local time stepping and implicit residual smoothing are used to accelerate the convergence rate. Wall boundary conditions are implemented on non-moving mean wall positions, meanwhile the first-order approximate boundary conditions are used in Euler equations on stationary Cartesian grids. This method needn't generate the deforming grids during calculation, thus it needs less demand on CPU time and can be easily deployed in any fluid-structure interaction problem.

2 Governing Equations

The two-dimensional unsteady Euler equations in conservative integral form in the Cartesian coordinate system (*x*,*y*) are

$$\frac{\partial}{\partial t}\int_V \boldsymbol{W} \mathrm{d}V + \int_S \boldsymbol{F}\cdot\boldsymbol{n}\mathrm{d}S = 0 \tag{1}$$

where

$$\boldsymbol{W} = \begin{bmatrix} \rho \\ \rho u \\ \rho v \\ \rho E \end{bmatrix} \tag{2}$$

$$\boldsymbol{F} = \begin{bmatrix} \rho(\boldsymbol{q}-\boldsymbol{q}_b) \\ \rho u(\boldsymbol{q}-\boldsymbol{q}_b) + p\boldsymbol{e}_x \\ \rho v(\boldsymbol{q}-\boldsymbol{q}_b) + p\boldsymbol{e}_y \\ \rho E(\boldsymbol{q}-\boldsymbol{q}_b) + p(u\boldsymbol{e}_x + v\boldsymbol{e}_y) \end{bmatrix} \tag{3}$$

$$\boldsymbol{q} = u\boldsymbol{e}_x + v\boldsymbol{e}_y \tag{4}$$

$$\boldsymbol{q}_b = u_b\boldsymbol{e}_x + v_b\boldsymbol{e}_y \tag{5}$$

$$E = \frac{1}{\gamma-1}\frac{p}{\rho} + \frac{1}{2}\left(u^2+v^2\right) \tag{6}$$

where ρ, p, $\boldsymbol{q}$, E, H represent density, pressure, velocity vector, total specific energy and total specific enthalpy respectively. u and v denote the *x* and *y* components of flow velocity.

Applying (1) to each cell in the mesh we obtain a set of ordinary differential equations of the form.

$$\frac{\mathrm{d}}{\mathrm{d}t}\left(\boldsymbol{W}_{i,j}V_{i,j}\right) + \mathbf{R}\left(\boldsymbol{W}_{i,j}\right) = 0 \tag{7}$$

where $V_{i,j}$ is the volume of the i, j cell and the residual $\mathbf{R}(\boldsymbol{W}_{i,j})$ is obtained by evaluating the flux integral in (1). Following Jameson[10], we approximate the *d/dt* operator by an implicit backward difference formula of second-order accuracy in the following form (dropping the subscripts).

$$\frac{3}{2\Delta t}\left[\boldsymbol{W}^{n+1}V^{n+1}\right] - \frac{2}{\Delta t}\left[\boldsymbol{W}^{n}V^{n}\right] + \frac{1}{2\Delta t}\left[\boldsymbol{W}^{n-1}V^{n-1}\right] + \mathbf{R}\left(\boldsymbol{W}^{n+1}\right) = 0 \tag{8}$$

Equation (8) can be solved for W^{n+1} at each time step by solving the following steady-state problem in a pseudo time t^*.

$$\frac{\mathrm{d}\boldsymbol{W}}{\mathrm{d}t^*} + \mathbf{R}^*\left(\boldsymbol{W}\right) = 0 \tag{9}$$

where

$$\mathbf{R}^*(\boldsymbol{W}) = \mathbf{R}(\boldsymbol{W}) + \frac{3}{2\Delta t}\left(\boldsymbol{W}V^{n+1}\right) - \frac{2}{\Delta t}\left(\boldsymbol{W}^{n}V^{n}\right) + \frac{1}{2\Delta t}\left(\boldsymbol{W}^{n-1}V^{n-1}\right) \tag{10}$$

Equation (9) is solved by an explicit time-marching scheme in t^* for which the local time stepping, residual smoothing can be used to accelerate convergence to a steady state solution.

,3 Approximate Boundary Conditions

A thin airfoil slightly moving around its mean position is considered. In this paper, the airfoil is assumed to be rigid and undergoes pitching or plunging motion around a fixed point on its chord line. The mean position of the airfoil chord lies on the horizontal axis x of the coordinate system. The shape of the airfoil is described by *y=f(x)*. The instantaneous position of the airfoil is described by *y=G(t,x)*. Under the assumption, *|F|<<1*, the first-order approximate of the boundary conditions on the surface of the airfoil at an instant *t* is

$$v(t,x,0) = u(t,x,0)F_x + F_t + O(F) \tag{11}$$

where the subscripts, x and t denote the partial derivatives with respect to *x* and *t*, respectively.

There are altogether four independent variables in the Euler equations (1), e.g. ρ, u, v and *p*. In addition to the boundary condition for the velocity component v given above, more conditions are needed on the airfoil surface. The momentum differential equation in the outward normal direction $\boldsymbol{n}$ is also used, which gives

$$\boldsymbol{n}\cdot\left[\frac{\partial\boldsymbol{q}}{\partial t} + \left(\boldsymbol{q}\cdot\nabla\boldsymbol{q}\right)\right] = \boldsymbol{n}\cdot\left(-\frac{\nabla p}{\rho}\right) \tag{12}$$

the above equation becomes

$$\begin{aligned} p_y(t,x,F) = {} & F_x p_x(t,x,F) - \rho(t,x,F) \\ & \left[F_{tt} + 2F_{tx}u(t,x,F) + F_{xx}u^2(t,x,F)\right] \end{aligned} \tag{13}$$

The first-order approximation of equation (13) is

$$p_y(t,x,\mathbf{0}) = F_x p_x(t,x,\mathbf{0}) - \rho(t,x,\mathbf{0}) \left[F_{tt} + 2F_{tx}u(t,x,\mathbf{0}) + F_{xx}u^2(t,x,\mathbf{0})\right] \quad (14)$$

For the airfoil pitching, the instantaneous angle from the mean position is $\alpha_1(t)$, positive in clockwise direction. Given *f(x),* the instantaneous ordinate of the surface, $F(t,x)$, is expressed implicitly as follows.

$$F\cos\alpha_1 + (x - x_0)\sin\alpha_1 = f\left[x_0 + (x - x_0)\cos\alpha_1 - F\sin\alpha\right] \quad (15)$$

Under the airfoil being thin and undergoing small deformation, the five derivatives of $F(t,x)$ used in equation (11) and (14) can be obtained from equation (15)

$$\begin{aligned} F_x &= f' - \tan\alpha_1 + O(F^3) \\ F_{xx} &= f'' + O(F^3) \\ F_t &= -\alpha_1'(x - x_0)\sec^2\alpha_1 + O(F^3) \\ F_{tx} &= -\alpha_1'\sec^2\alpha_1 + O(F^3) \\ F_{tt} &= -(x - x_0)\sec^2\alpha_1\left(\alpha_1'' + 2\alpha_1'^2\right) + O(F^3) \end{aligned} \quad (16)$$

where the $'$ denotes differentiation of $f(x)$ and $\alpha(t)$ with respect to x and t ,respectively.

3 Structural Solver

The second-order linear structural dynamic governing equation of motion can be written as

$$\boldsymbol{M}\ddot{\mathbf{z}} + \boldsymbol{C}\dot{\mathbf{z}} + \boldsymbol{K}\mathbf{z} = \boldsymbol{F} \quad (17)$$

where $\boldsymbol{M}$, $\boldsymbol{C}$ and $\boldsymbol{K}$ are mass, damping and stiffness matrices, respectively. $\mathbf{z}$ is displacement vector, and $\boldsymbol{F}$ is the aerodynamic load.

In this study, the data of natural mode shapes and frequencies are calculated by finite-element analysis. In order to solve equation (17), the generalized displacement, $\boldsymbol{\eta}$, is introduced.

$$\mathbf{z} = [\phi]\boldsymbol{\eta} \quad (18)$$

Since the natural modes are orthogonal with respect to both the mass and stiffness matrices, premultiplying equation (17) by $[\phi]^T$ yields structural equations in generalized coordinates

$$\ddot{\eta}_i + 2\zeta_i\omega_i\dot{\eta}_i + \omega_i^2\eta_i = Q_i \quad (19)$$

where $Q_i = \{\phi\}_i^T F$, $\omega_i^2 = \{\phi\}_i^T \boldsymbol{K}\{\phi\}_i$, $1 = \{\phi\}_i^T \boldsymbol{M}\{\phi\}_i$ and ζ_i is the modal damping of the ith mode.

At a time $t + \Delta t$, equation (16) can be written as

$$\ddot{\eta}_{i\,t+\Delta t} + 2\zeta_i\omega_i\dot{\eta}_{i\,t+\Delta t} + \omega_i^2\eta_{i\,t+\Delta t} = Q_{i\,t+\Delta t} \quad (20)$$

In the above expression, ω_i , ζ_i and $Q_{i\,t+\Delta t}$ are already known. So we can obtain the displacement, velocity and acceleration at $t + \Delta t$ by using the Newmark integration method. The following expressions for velocity and displacement are formulated at the time $t + \Delta t$ first as a function of acceleration at $t + \Delta t$ and displacement, velocity and acceleration from previous time level t .

$$\dot{\eta}_{i\,t+\Delta t} = \dot{\eta}_{i\,t} + \left[(1-\delta)\ddot{\eta}_{i\,t} + \delta\ddot{\eta}_{i\,t+\Delta t}\right]\Delta t \quad (21)$$

$$\eta_{i\,t+\Delta t} = \eta_{i\,t} + \dot{\eta}_{i\,t}\Delta t + \left[\left(\frac{1}{2} - \alpha\right)\ddot{\eta}_{i\,t} + \alpha\ddot{\eta}_{i\,t+\Delta t}\right]\Delta t^2 \quad (22)$$

where, α and δ are parameters that are chosen based on desired stability and accuracy. For the Newmark scheme to be unconditionally stable, values of 0.25 and 0.5 are chosen for α and δ , respectively.

4 Results and Discussion

4.1 Unsteady Flow Calculation

The flow over NACA 64A010 airfoil is calculated using the first-order approximate conditions. The airfoil foil is pitching around its quarter-chord point. Experimental results were provided by Davis[11]. The harmonic pitching motion of the airfoil can be described by the following equation

$$\alpha(t) = \alpha_m + \alpha_0\sin(\omega t) \quad (23)$$

where ω , α_m and α_0 are constants. The angular frequency ω is related to the reduced frequency defined as

$$k = \frac{\omega c}{2U_\infty} \quad (24)$$

In this case, the free stream Mach number is $Ma = 0.796$, and the mean angle of attack $\alpha_m = 0.0^\circ$, the pitching amplitude $\alpha_0 = 1.01^\circ$ and the reduced frequency $k = 0.202$. The unsteady calculations start from the uniform flow of velocity U_∞ as an initial solution. An essentially periodic solution is obtained after certain periods of the airfoil motion. Fig.1. compares the lift and moment coefficients versus angle of attack with the experimental results. It is shown that the solution by the approximate boundary conditions is sufficiently close to the experimental results. We can conclude that the first-order approximate boundary conditions are suitable for solution of the transonic unsteady Euler equations.

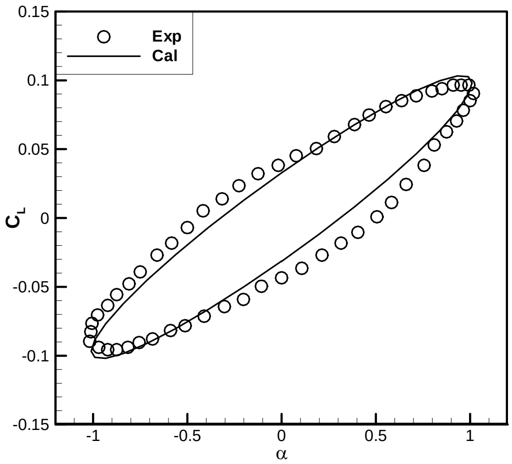

(a) Lift Coefficient

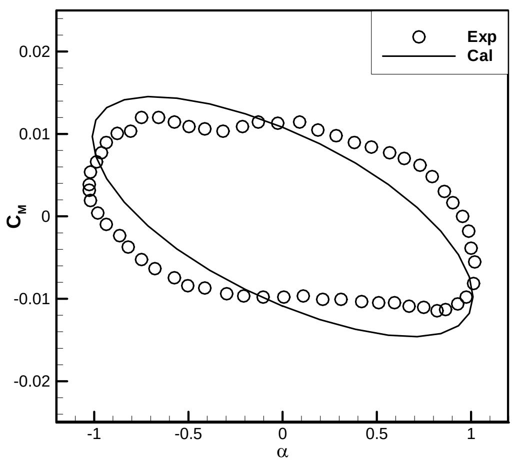

(b) Moment Coefficient

Fig.1. Time Histories of Lift and Moment Coefficient of NACA64A010

4.2 Flutter Calculation

In this section, we use the present method to predict flutter boundaries of Isogai wing model and NACA 0012 benchmark model. The elastic model is established as shown in Fig.2, which consists of two degrees of freedom, plunging and pitching.

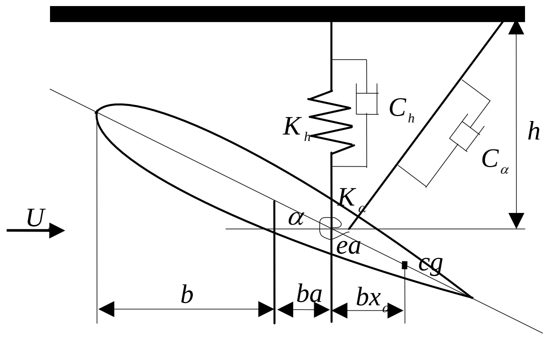

Fig.2. Isogai Wing Model

In order to obtain the flutter boundary, different speed index V^* are computed. V^* is defined as

$$V^* = \frac{U_\infty}{b\omega_\alpha\sqrt{\mu}} \tag{25}$$

b is the airfoil half chord.

4.2.1 Isogai Wing Model

In this section, we use approximate method coupled equation of structural motion for the two-dimensional Isogai wing model[12,13], case A. this model is well established 2-analog of a 3-D wing. The cross-section profile of this model is NACA 64A010 airfoil. The structural parameters are: $a = -2.0$, $x_\alpha = 1.8$, $r_\alpha^2 = 3.48$, $\omega_h/\omega_\alpha = 1.0$ and $\mu = 60$. In this test case, the model simulates the bending and torsional motion of a wing cross-section in the outboard portion of a swept wing.

Fig.3. shows the time history of plunging and pitching motion of Isogai wing model at the Mach number of *Ma*=0.875. In Fig.3, the amplitude of plunging and pitching motion keeps constant at the speed index *V**=0.590. So the speed index of this neutral point is the flutter velocity at *Ma*=0.875. We can obtain the critical velocity for a number of freestream Mach

numbers for the Isogai wing model in the same

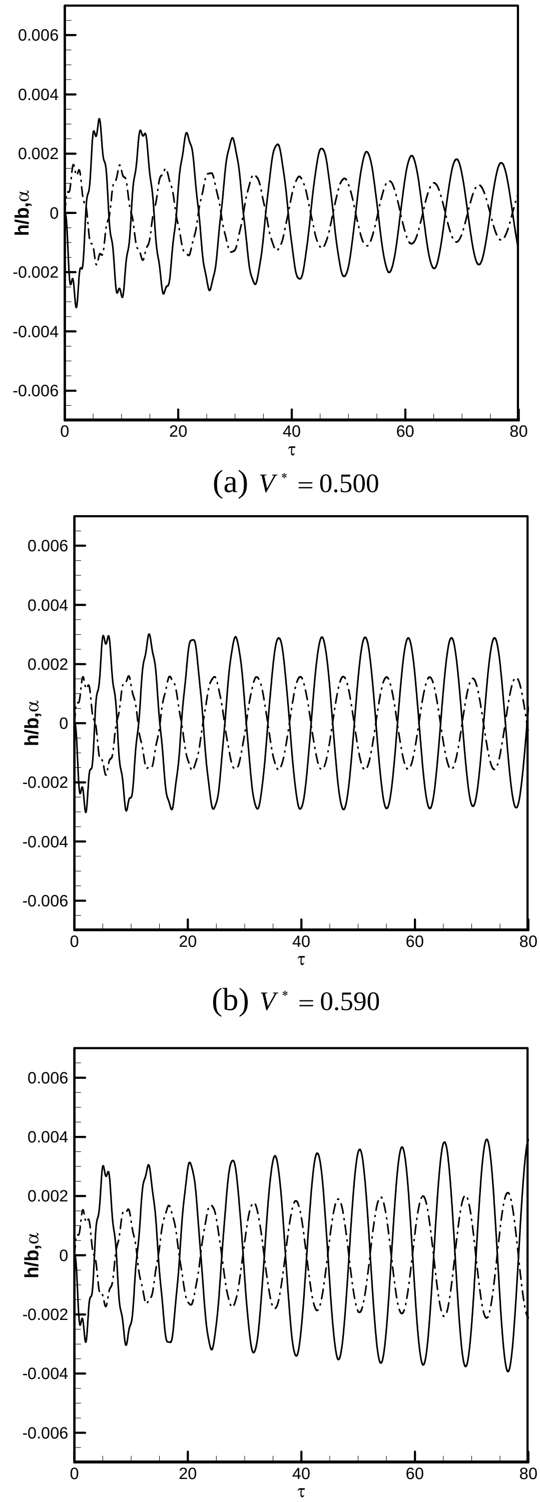

(a) $V^* = 0.500$

(b) $V^* = 0.590$

(c) $V^* = 0.630$

Fig.3. Time History of Plunging and Pitching motion of Isogai Model at *Ma=0.875*

way. The flutter boundary is predicted by the unsteady Euler Equations on stationary Cartesian grid with the first-order approximate conditions is shown in Fig.4, and compared with the results of Alonso[5] and Liu[6]. The agreement is good and the transonic "dip" is predicted accurately. The results show that the first-order approximate conditions on the stationary Cartesian grids can predict the flutter boundary as those accurate boundary conditions.

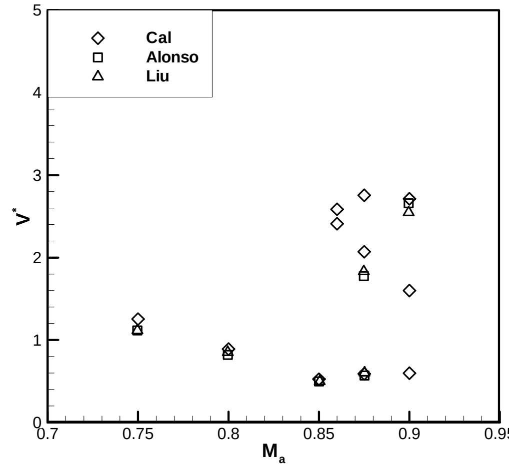

Fig.4. Computed Flutter Boundary of the Isogai Wing Model

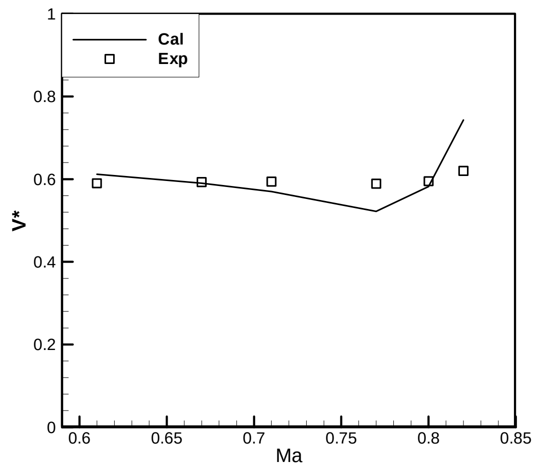

Fig.5. Conventional Flutter Boundary of NACA 0012 Benchmark Model

4.2.1 NACA0012 Benchmark Model

The model is a semispan rigid wing mounted on a flexible mount system referred to as the Pitch and Plunge Apparatus (PAPA). The model has a NACA 0012 airfoil section and a rectangular planform with a span of 32 inches and a chord of 16 inches. Rivera et al.[14] performed flutter experiments for this benchmark model.

According to Ref.14, the system center of gravity was adjusted to be right on the PAPA elastic axis which was located at the mid-chord line. Therefore, the structural parameters are: $a=0$, $x_{\alpha}=0$, $r_{\alpha}^{2}=1.0236$, $\omega_{h}/\omega_{\alpha}=0.6462$.

The comparison of calculated and experimental conventional flutter boundaries is shown in Fig.5. Overall, the computed results are in good agreement with the experimental data. The “transonic dip” is captured by the computation using first-order approximate boundary conditions. However, the difference between computed and experimental results becomes more seriously beyond the “transonic dip” region.

5 Conclusion

In this paper, we use the first-order approximate boundary conditions to solve the unsteady Euler equations coupled with equations of structural motion on stationary Cartesian grids. Using this approximate method, we solve the two dimensional unsteady flow around NACA 64A010, and two aeroelastic cases for Isogai wing model and NACA 0012 benchmark model. Both the results of unsteady transonic calculation and aeroelastic calculation are in good agreement with related references, preliminarily indicating that the first-order approximate conditions are effective for aeroelastic simulation.

References

[1] Bendiksen O O and Kousen K A. Transonic flutter analysis using the Euler equation. AIAA Paper 1987-0911, 1987.

[2] Kousen K A and Bendiksen O O. Limit cycle phenomena in computational transonic aeroelasticity. *Journal of Aircraft*, Vol. 31, No. 6, pp 1257-1263, 1994.

[3] Lee-Rausch E M and Batina J T. Wing flutter boundary prediction using unsteady Euler aerodynamic method. *Journal of Aircraft*, Vol. 32, No. 2, pp 416-422, 1995.

[4] Lee-Rausch E M and Batina J T, Wing flutter computations using an aerodynamic model based on the Navier-Stokes equations. *Journal of Aircraft*, Vol. 33, No. 6, pp 1139-1147, 1996.

[5] Alonso J J and Jameson A. Fully- implicit time-marching aeroealstic solutions. AIAA Paper 1994-0056, 1994.

[6] Liu F, Cai J and Zhu Y, Calculation of wing flutter by a coupled fluid-structure method. *Journal of Aircraft*, Vol. 38, No. 2, pp 334-342, 2001.

[7] Gao C, Luo S and Liu F. Calculation of unsteady transonic flow by an Euler method with small perturbation boundary conditions. AIAA 2003-1267, 2003.

[8] Gao C, Luo S, Liu F and Schuster D M. Calculation of airfoil flutter by an Euler method with approximate boundary conditions. AIAA 2003-3830, 2003.

[9] Zhang Y H. *Numerical simulations of transonic flow of wing by solving Euler equations with approximate boundary method*. Northwestern Polytechnical University, 2005.

[10] Jameson A. Time dependent calculations using multigrid, with applications to unsteady flows past airfoils and wings. AIAA Paper 1991-1596, 1991.

[11] Davis S S. NACA 64A010 oscillatory pitching, compendium of unsteady aerodynamics measurements. AGARD Report 702, 1982.

[12] Isogai K. On the transonic-dip mechanism of flutter of a sweptback wing. *AIAA Journal*, Vol. 17, No. 7, pp 793-795, 1979.

[13] Isogai K. Transonic dip mechanism of flutter of a sweptback wing: part II. *AIAA Journal*, Vol. 19, No. 9, pp 1240-1242, 1981.

[14] Rivera J A. NACA 0012 benchmark model experimental flutter results with unsteady pressure distributions. NASA TM-107581, 1992.

Copyright Statement